Journal of Materials Chemistry B

Accepted Manuscript

ROYAL SOCIETY OF CHEMISTRY

www.rsc.org/materialsB

Cite this: DOI: 10.1039/c0xx00000x

www.rsc.org/xxxxxx

ARTICLE TYPE

Mesoporous Silica Nanoparticles for Glutathione-Triggered Long-Range and Stable Releasing Hydrogen Sulfide

Xiaotian Sun[a,b†], Biao Kong[c,d†], Wenshuo Wang[a], Paurnami Chandran[d], Cordelia Selomulya[d], Huili Zhang[e], Kai Zhu[a], Ye Liu[f], Wuli Yang[f], Changfa Guo[a]*, Dongyuan Zhao[c,d] and Chunsheng Wang[a]*

Received (in XXX, XXX) Xth XXXXXXXXX 20XX, Accepted Xth XXXXXXXXX 20XX
DOI: 10.1039/b000000x

Mesoporous silica nanoparticles (MSNs) that can stably load therapeutic drugs and release them in response to a specific trigger are of great interest in disease diagnosis and treatment. However, the controlled-release of gaseous drug molecules such as hydrogen sulfide (H_2S) from a long-range, stable MSN-based system still presents a great challenge. Herein, a MSN-based glutathione (GSH)-triggered controlled-release H_2S system has been fabricated, with high entrapment efficiency (99.0 ± 0.3%) and loading content (44.2 ± 0.1%) of diallyl trisulfide (DATS). After the addition of GSH (2 mM), DATS-MSN (100 μg/mL) releases moderate amounts of H_2S steadily (peaking at the 4th hour, ~ 60 μM) in phosphate buffer solution (PBS). The release of H_2S in plasma is similar to a physiological process (peaking at the 4th hour) and the DATS-MSN remains in the plasma of rat's system over 9 hours without significantly affecting the blood pressure, heart rate and cardiac function. Moderate quantities of nanoparticles can be taken up by cardiomyocytes in vitro, while in vivo study shows that nanoparticles mainly accumulate in liver and spleen, affecting the H_2S level in these organs. Furthermore, DATS-MSN shows excellent biocompatibility, as well as superior cytoprotection and isolated heart protection effect of H_2S under ischemic/reperfusion injury. This study provides a new insight into controlled-release applications of MSN-based H_2S releasing systems both in vitro and in vivo.

Introduction

Mesoporous silica nanoparticles are one of the most promising and versatile drug carrier candidates which meet the need of ideal nanovehicles.[1-5] Drugs delivered by MSNs showed several advantages compared to free drugs, such as improved solubility, stability, therapeutic efficacy, and biocompatibility.[6-10] Despite these promising benefits, the release of gas molecule drugs from the MSN frameworks in a controlled fashion still present a challenge. Stimuli-responsive MSN-drug formulations have a great potential to solve this problem due to their unique response to specific triggers. Examples of the most widely used intracellular or extracellular stimuli in the design of stimuli-responsive MSNs include pH, redox potential, light, temperature, and enzyme.[11-14] These smart drug delivery systems are designed to release their payloads at targeted organelles and tissues for *in vitro* and *in vivo* applications, respectively.[15-17]

In recent years, hydrogen sulfide (H_2S) has been recognized as the most common gaseous transmitter along with nitric oxide (NO) and carbon monoxide (CO). H_2S is endogenously synthesized from cysteine activated by several enzymes such as cystathionine β-synthase (CBS), cystathionine γ-lyase (CSE), and 3-mercaptopyruvate sulfur-transferase (3-MST). The gaseous transmitter provides various physiological and pathophysiological effects in different tissues, especially in the cardiovascular system. For example, H_2S can exert cytoprotection and anti-apoptotic effects by attenuating ischemia reperfusion injury in myocardium, preserving cardiac function.[18, 19] Besides, H_2S also provides vasodilation and anti-hypertensive effects by opening adenosine triphosphate sensitive potassium channels of vascular smooth muscles cells.[20] Furthermore, H_2S is also involved in many physiological processes including anti-inflammation,[21] antioxidant defense responses,[22] neuromodulation,[23] inhibiting insulin resistance,[24] atherogenesis,[25] anti-platelet activation,[26] and metabolic suppression,[27] Underlying mechanisms of these biological functions are being under studied with increasing interest.

H_2S studies have nowadays been largely promoted by realising ideal H_2S donors. Previous studies employed many different H_2S donors with different features. Sodium hydrosulfide (NaHS), the most commonly used H_2S donor, can rapidly increase H_2S concentration. However the instant release of H_2S cause many adverse effects in the body such as rapid fall in blood pressure,[28] and it cannot mimic the slow and continuous process of H_2S generation *in vivo*. Morpholin-4-ium 4 methoxyphenyl (morpholino) phosphinodithioate (GYY4137), a derivative of Lawesson's reagent, can slowly release H_2S in aqueous solution,[29] but the H_2S concentration is relatively low and the release is uncontrollable. Cysteine analogs including S-propyl cysteine (SPC), S-allyl cysteine (SAC) and S-propargyl cysteine (SPRC) could act as endogenous H_2S donors and increase both

the quantity and rate of H_2S production *in vivo*,[30] but this process is hardly regulated and not suitable for various *in vitro* studies of H_2S. A class of cysteine-activated H_2S donors has been developed recently,[31, 32], and moderate amounts of H_2S can be slowly released in the presence of excess cysteine, but little biological studies of these donors have been reported to date. Nowadays, diallyl trisulfide (DATS), which is obtained from the decomposition of garlic-derived polysulfide compounds in water, along with diallyl sulfide (DAS) and diallyl disulfide (DADS),[33] has drawn great attention as a potential H_2S donor. H_2S could be generated from these decomposition products in the presence of thiols such as reduced GSH both in red blood cells and in phosphate buffers (PBS). The mechanism mainly involves typical thiol/disulphide exchange and employs GSH as a nucleophilic substituent on the alpha carbon. GSH itself does not serve as H_2S donors, but converts into oxidized glutathione (GSSG) in the reaction process.[34] Among these decomposition products, DATS has the most tethering sulfur atoms and H_2S production, while some of its beneficial effects in cardiovascular and neurological diseases are also derived from H_2S.[35] However, the poor solubility of DATS in aqueous media limits its use as the H_2S donor, and its H_2S release is still relatively fast *in vitro* after the addition of GSH. To date, DATS-based H_2S release still calls for an ideal H_2S donor releasing H_2S slowly and controllably, which can mimic the physiological process.

To control the H_2S release from the existing H_2S donors, mesoporous silica nanoparticle has been considered as the ideal carrier in this study. MSN is an ideal drug carrier due to its attractive features such as large surface area and pore volume, easily modified pore sizes, good biocompatibility, diverse surface functionality, [1, 2, 16] as well as its good dispersity in aqueous medium, which can reformulate poorly water-soluble drugs.[7, 8] Furthermore, MSN can prolong the *in vivo* circulation time of the loaded drugs safely.[10, 16, 17] As mentioned above, the several features, GSH triggered smart releasing, abundant sulfur atoms for H_2S generation, and proper molecular weight (178 g/mol) for loading, enable DATS as an ideal loaded drug superior to other traditional H_2S donors. Therfore the aim of the study is to exploit MSN as the carrier of DATS, by synthesising a GSH-activated, water-dispersible, slow and controllable H_2S-releasing system (DATS-MSN). The mechanisms of DATS molecules escaping from the mesopores of nanoparticles and/or GSH molecules entering the pores to slow down the reaction to generate H_2S are proposed. The H_2S release manner of the new system compared with previous H_2S donors are investigated *in vitro* and *in vivo*. It is of great interest to elucidate whether the long-range and stable releasing donor causes the better biofunctionality of H_2S. It is also necessary to identify the biocompatibility of DATS-MSN, as well as its ability of being captured by cells and different organs, which would affect H_2S distribution *in vivo*. The study provides a unique MSN-based platform for controlled release of H_2S *in vitro* and *in vivo*.

Results

Characterization of DATS-MSN

Transmission electron microscopy (TEM) images indicate mesoporous silica nanoparticles are monodisperse with uniform size and regular mesopores **(Fig. 1a, b)**. The diameter of MSN is ~ 225 ± 35 nm (n = 3). The Brunauer, Emmett and Teller (BET) surface area of the MSNs is measured to be ~ 813 m^2/g (**Fig. 1c**). The pore size distribution curve (**Fig. 1d**) indicates that the obtained MSN has uniform pore size of ~ 2 nm. As was shown in **Fig. S1**, the hydrodynamic diameter for DLS test is ~ 289 nm (PDI = 0.08). Due to the high superficial area and interaction between DATS and Si-OH, the entrapment efficiency of DATS-MSN is ~ 99.0 ± 0.3% (n = 3), suggesting that overwhelming majority of drugs is combined to MSN. The calculated drug loading contents of the samples are ~ 44.2 ± 0.1% (n = 3). As shown in **Fig. S2,** the content of DATS released in 24 h is relatively low at ~ 8.4 ± 1.1% (n = 3).

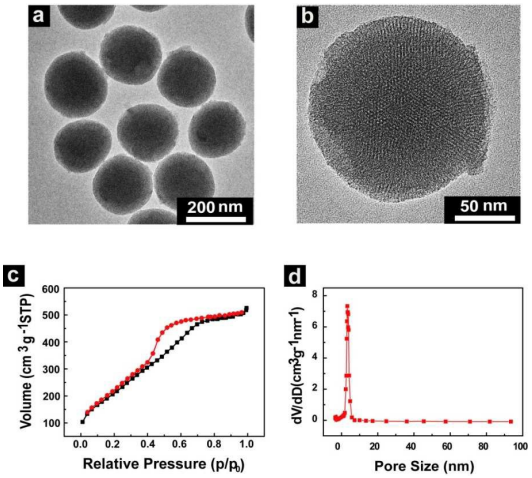

Fig. 1. Characterization of DATS-MSN. (**a,b**) TEM (a) and enlarged TEM (b) images. (**c,d**) Surface area measurement (c) and pore distribution (d) by multipoint BET analysis.

In vitro H_2S release of DATS-MSN

DATS-MSN released moderate amounts of H_2S in PBS steadily, which can be regulated by GSH concentration and pH condition (**Fig. 2a**). DATS and DATS-MSN are both stable in PBS (100 mM, pH 7.4) as shown by H_2S-selective microelectrode. After adding 2 mM GSH, different H_2S release curves are observed for the two systems. The release of H_2S from DATS-MSN is much slower and continuous. The curve still continues to rise after 80 min. In contrast, DATS releases H_2S relatively rapidly, peaking at about 35 min before starting to fall. Compared to the peak, the real time picoamps current shows a significant decline after more than 1 h. As a control, H_2S generation from NaHS is also quite rapid. The concentration instantly peaks in seconds and rapidly decreases nearly to the baseline after half an hour without reaching a plateau.

For high-performance liquid chromatography (HPLC) analysis, H_2S generation of DATS-MSN in PBS (100 mM, pH 7.4) with GSH is shown in **Fig. 2b**. The maximum value is reached at the 4th hour (peaking time), while the plateau time is between 2-6 h, after which the H_2S concentration decreases gradually. In the presence of different concentrations of GSH, DATS-MSN releases significantly different amounts of H_2S. H_2S concentrations are apparently reduced by the decrease of GSH concentration from 2 mM, 200 μM to 20 μM (**Fig. 2b**). The

release of H_2S from DATS-MSN is pH dependent (**Fig. 2c**) as it is significantly inhibited in an acidic (pH 6.5) compared with neutral (pH 7.4) environment, while alkaline PBS (pH 8.0) did not apparently affect H_2S release. Temperatures (37, 20 and 4 °C) have negligible impacts on generation and release of H_2S (**Fig. 2d**).

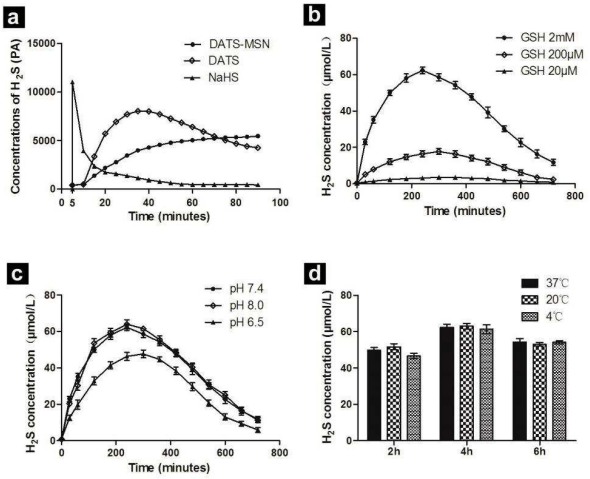

Fig. 2. Release of H_2S from DATS-MSN in PBS solution. (**a**) DATS (10 μg/mL), DATS-MSN (10 μg/mL) and NaHS (10 μM) with GSH (2 mM) (pH 7.4, 37 °C). Drugs are added at 5th min, and GSH is added at the 10th min. (**b**) DATS-MSN (100 μg/mL) with different concentrations of GSH (2 mM, 200 μM and 20μM) at pH 7.4 and 37 °C. (**c**) DATS-MSN (100 μg/mL) in different pH (8.0, 7.4 and 6.5) with GSH (2mM) at 37 °C. (**d**). DATS-MSN (100 μg/mL) with different temperatures (37 °C, 20 °C and 4 °C) at time point 2, 4 and 6 h with GSH (2 mM) at pH 7.4. (a) Measurements are assessed by H_2S-selective microelectrode, and representative tracings are obtained by at least 6 similar measurements. (b-d) Measurements are performed by HPLC method (mean ± SEM, n = 6).

Cytotoxicity assays and in vitro cellular uptake

DATS-MSN shows no significant toxicity (cell viability > 80%) even at the concentration up to 100 μg/mL (**Fig. 3a**), suggesting that it can be safely used as H_2S donor *in vitro*. Orange fluorescence of Cyanine 3 labelled MSN (Cy3-MSN) is observed in cytoplasm, proving that the nanoparticles are phagocytized by cardiomyocytes successfully (**Fig. 3b,c**). The fluorescent intensity of the nanoparticles is proportional to their number concentration, and a moderate concentration in cardiomyocytes was observed.

Protection effect of DATS-MSN from hypoxia/reoxygenation induced damage

Cell counting kit-8 (CCK-8) assay indicates that cell viability is protected by all NaHS, DATS and DATS-MSN pretreatment compared with control after hypoxia/reoxygenation procedure, however, this protection effect in DATS-MSN group is significantly better than in either NaHS or DATS group (**Fig. 3d**). The lactate dehydrogenase (LDH) activity measurement shows that LDH activity is the lowest in DATS-MSN group after the hypoxia/reoxygenation procedure (**Fig. 3e**), although a decrease of LDH activity is observed in all pretreating groups.

***In vivo* H_2S release of DATS-MSN in plasma**

H_2S release from DATS-MSN in plasma *in vivo* is slow and mimics the physiological process. After vein injection of DATS-MSN, H_2S concentration in rat plasma increases from the first time point (30 min), peaks at the 4th hour, and remains increasing over 9 h experiment. In contrast, although NaHS apparently increases the plasma H_2S concentration soon after administration (peaking at 1 h), H_2S levels reduces to baseline after 3 h. Direct administration of the same amount of DATS shows a smaller increase of H_2S concentration and shorter affecting time than that of DATS-MSN (**Fig. 3f**).

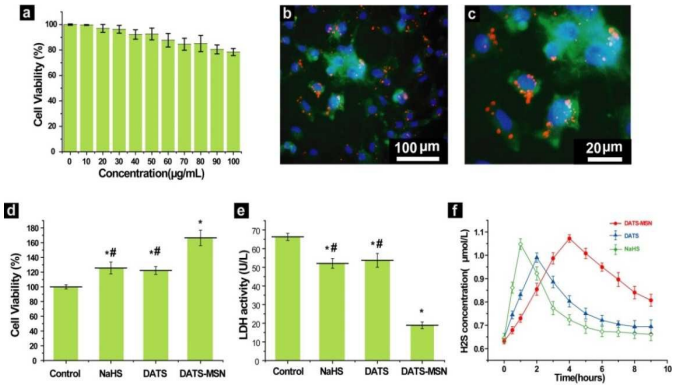

Fig. 3. DATS-MSN with neonatal rat cardiomyocytes and H_2S release in plasma. **(a)** Cell viability after incubated for 24 h in different concentrations of DATS-MSN (mean ± SEM, n = 3). **(b,c)** Fluoresce microscopic images after 4 h incubation with Cy3-MSN (50 μg/mL). Orange: Cy3-MSN, Green: cytoplasm stained by phalloidin, Blue: nucleus stained by DAPI. **(d,e)** Cell viability (d) and Lactate dehydrogenase (LDH) activity (e) after a 4 h hypoxia and 1 h reoxygenation procedure pretreated in DATS-MSN (100 μg/mL) + GSH (2 mM), DATS (100 μg/mL) + GSH (2 mM), NaHS (100 μM) and control (mean ± SEM, n = 3). *: P<0.05 compared with Control, : P<0.05 compared with DATS-MSN group. **(f)** H_2S concentration in plasma after tail vein injection of NaHS (100 μmol/kg), DATS (10 mg/kg) and DATS-MSN (10 mg/kg) (mean ± SEM, n = 6).

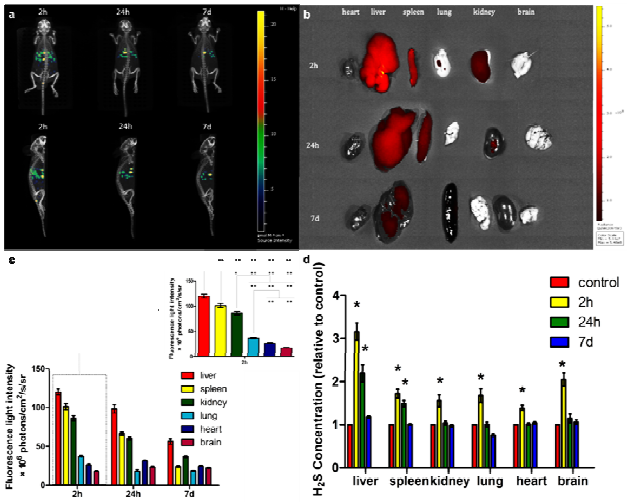

Fig. 4. Biodistribution of DATS-MSN and H_2S at 2 h, 24 h and 7 d after injection of CY7-MSN or DATS-MSN. **(a)** 3D reconstruction of FLIT for nude mice (prone and right side position) after injection of CY7-MSN (5 mg/kg). **(b)** Heart, liver, spleen, lung, kidney and brain of rats for ex vivo imaging after injection of CY7-MSN (5 mg/kg). **(c)** Quantitative analysis of fluorescence intensities of individual organs of (b). (mean ± SEM, n = 6, *: $P < 0.05$). **(d)** H_2S concentration in heart, liver, spleen, lung, kidney and brain of rats after injection of DATS-MSN 10 mg/kg. (mean ± SEM, n = 6, *: $P < 0.05$ compared with the control group of the same organ).

Biodistribution of DATS-MSN and H_2S in organs

3D reconstruction of Fluorescence Light Imaging Tomography (FLIT) shows that nanoparticles in the mice body are mainly detected in the region of liver, spleen and kidney, indicating the accumulation of nanoparticles in these organs (**Fig. 4a**). The fluorescence signal intensity peaks at 2 h, followed by a gradual decrease at 24 h and 7 d. At 7 d, the mice body only contains slight fluorescence signals. Rat *ex vivo* fluorescence imaging shows similar results. After euthanasia at 2 h, 24 h and 7 d after DATS-MSN administration, the fluorescence signals of liver, kidney, spleen, lung, heart and brain collected are shown in **Fig. 4b**. The strongest fluorescence signal intensity is observed at 2 h, mainly detected in liver, spleen and kidney, maintaining high levels for at least 24 h. At 7 d, the fluorescence signals of these organs almost decrease to the same level as the whole body except for slight enhancement in liver (**Fig. 4c**). Compared to the control, H_2S contents in liver, kidney, spleen, heart, lung and brain are all clearly elevated at 2 h, especially in liver (**Fig. 4d**). The H_2S content in organs decreases in a time-dependent way. At 24 h after injection, H_2S level in just the liver and spleen has a slightly higher than that in control. At 7 d, H_2S content in all organs falls back to the control level.

Effect of DATS-MSN on blood pressure, heart rates and cardiac function

DATS-MSN makes little difference to either mean artery pressure or heart rates within 1 h (**Fig. S3**). In contrast, NaHS causes immediate and time-dependent fall in the rat's mean artery pressure in 1 h (**Fig. S3a**). Furthermore, heart rates are inhibited by NaHS administration but not by DATS-MSN (**Fig. S3b**). Neither NaHS nor DATS-MSN shows obvious heart inhibition, with no significant difference in both cardiac structure (left ventricular end-diastolic volume and left ventricular end-systolic volume) and function (ejection fraction and fractional shortening) data compared to that in control (**Table 1**).

Hematological, serological and histological examinations

After injection with DATS-MSN for 2 h, 24 h and 7 d, all treated rats survived with normal activity. No abnormal symptom or behavior is observed. There is no visible erythema or necrosis at the injection regions. As shown in **Table 2**, at 2 h, 24 h and 7 d, there is no significant difference on the red blood cells (RBC), white blood cells (WBC), platelets (PLT), hemoglobin (HGB) and hematocrit (HCT) when comparing the DATS-MSN treated rats to those in the control group. Similarly, no difference in WBC distribution (neutrophils and lymphocytes) is observed between the control and treated animals. Meanwhile, the levels of indicators of hepatic and renal function including aspartate aminotransferase (AST), alanine aminotransferase (ALT), serum creatinine (CRE) and urea nitrogen in the serum (BUN) are all similar in DATS-MSN treated group and control group at each time point. As shown in **Fig. S4**, compared with the control, all tissues (liver, kidney spleen, heart, lung, and brain) show no obvious pathological change in hematoxylin and eosin (H&E) examination at 2 h, 24 h and 7 d after DATS-MSN injection, indicating that DATS-MSN causes no significant tissue toxicity.

Protection effect of DATS-MSN from ischemic/reperfusion (I/R) injury

The pretreatment of NaHS, DATS and DATS-MSN shows heart protection effect after I/R injury compared with control, however, the best functional recovery is observed in DATS-MSN group, with significantly greater left ventricle developed pressure (LVDP, systolic minus diastolic pressure), maximum rate of left ventricular pressure development (+dp/dt max, -dp/dt max) and coronary flow than those from either NaHS or DATS group (**Table 3**). Meanwhile, although less apoptotic cells proportion is observed, decreased LDH and creatine kinase (CK) levels in collected perfused buffers are demonstrated in all 3 pretreatment groups compared with that in the control. The effect is most significantly observed in DATS-MSN group (**Fig. S5**). These observations indicate that DATS-MSN provides the heart protection effect of H_2S in I/R injury, which is more effective than either NaHS or DATS.

Discussion

MSN is utilized to reformulate a natural H_2S donor—DATS, and to successfully synthesize a novel H_2S-releasing system activated by GSH. Unlike NaHS and free DATS, DATS-MSN can release moderate amounts of H_2S in a very slow and controllable way *in vitro*. It can also continually elevate H_2S levels in plasma and in major organs, the H_2S levels observed from *in vivo* studies are affected by the MSN distribution. The new system can thus be safely used, and effectively induce the biological functions of H_2S such as cyto and organ protection effect.

DATS-MSN shows good water dispersity, and presents a slow and continuous H_2S release, which is different from those of NaHS and free DATS. NaHS releases H_2S too rapidly, with a sharp initial increase and followed by a rapid decrease of H_2S concentration. Free DATS decomposes and generates H_2S more slowly than NaHS, but still relatively faster than DATS-MSN.

DATS-MSN slowly releases H_2S, which can be regulated by GSH concentration *in vitro*.

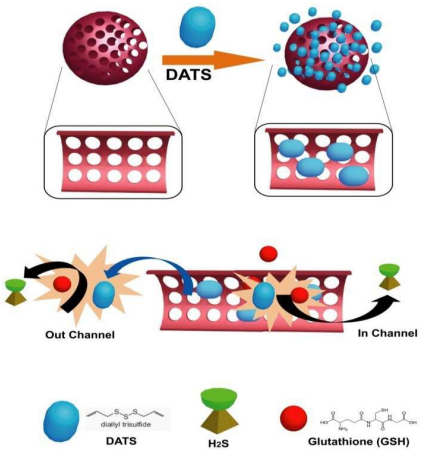

Fig. 5. A schematic illustration of the mechanism of H_2S slow-release from DATS-MSN.

For the release mechanism of DATS-MSN *in vitro*, DATS molecules may gradually be released into the solution and interact with GSH molecules for reaction. Our study shows that the content of DATS released from DATS-MSN is limited. So a possible mechanism could be that GSH molecules move into the mesopores of MSN to react with DATS for H_2S generation, which may slow down the release profile (**Fig. 5**). H_2S generation from DATS-MSN is a GSH-dependent pathway, limited by a lower GSH concentration. It suggests that H_2S release from the new system can be easily controlled by regulating GSH concentration, suitable for *in vitro* experiments requiring consistent but adjustable H_2S concentrations. The original intention of the study is to gain a slow-releasing H_2S donor applied to organ preservation solution. Therefore, besides the physiological temperature (37 ^oC) and room temperature (20 ^oC), the temperature for organ preservation (4 ^oC) has also been studied. Data shows that H_2S release is not inhibited at low temperature. On the other hand, H_2S production is apparently limited in an acidic environment.

For *in vivo* study and circulation of DATS-MSN, the DATS-MSN system can also be used as a H_2S donor *in vivo*. Compared with NaHS, DATS-MSN increases H_2S concentration in the bloodstream slowly. Although the GSH concentration is relatively low in plasma[36] (under 2 μM), the reduction of NADP+ to NADPH via pentose phosphate pathway (PPP), supported by glucose as the main energy source, maintains the GSH pool and ensures a sufficient GSH supply.[34] On the other hand, other biological thiols in plasma such as cysteine may compete with GSH for the DATS. The H_2S release profile in such complex environment could be quite different from that in aqueous solution. In addition, H_2S release *in vivo* also involves the distribution and metabolism of DATS-MSN. It has been reported[10] that the blood circulation lifetime of MSN with similar size (200 nm) was nearly 4 h. In this study, plasma H_2S concentration started to fall at 4 h after DATS-MSN injection, slower that clearance of MSN nanoparticles. The relatively large DATS-MSN particles (~ 225 nm) possess suitable blood-circulation lifetime and well controlled releasing rate of H_2S, which also demonstrate effectively exerting protective effect of H_2S. Without good dispersity and circulation effect of MSN, the administration of free DATS temporarily elevates plasma H_2S level which is insufficient. Therefore, combining with MSN makes DATS a more suitable H_2S donor in *in vivo* studies, and size modification and surface functionality of MSN in the future may bring more benefits.

For the uptake of MSN into cell, the clearance of MSN in blood circulation is mainly due to capture by various tissues, and intracellular uptake is one of the most important characters of nanoparticles. MSN can efficiently "enter" a variety of mammalian cells,[37] and it is observed in this study that moderate quantities of nanoparticles were taken up by cardiomyocytes *in vitro*. Endocytosing is an important way by which drugs are being delivered into targeted cells, especially for biological molecules that lack specific membrane-bound receptors. It has been reported that H_2S production from DATS molecule is largely mediated by exofacial membrane protein thiols but not by intracellular thiols,[34] the intracellular GSH concentration (2 mM) is much higher than that in the cellular exterior (2 μM).[36, 38] Thus the endocytosis process of MSN may trigger larger amounts of H_2S production from DATS and change the intracellular H_2S levels. For nanoparticles with size larger than 100 nm, smaller nanoparticles passes through the cytomembrane more easily in considerable quantity.[39] However, DATS-MSN is designed to be applied in a simple release environment, so the size of nanoparticles is relatively large and the intracellular process is controlled.

In accordance with previous studies that show nanoparticles taken up mainly by the reticuloendothelial system (RES) organs *in vivo*,[40] the distribution of DATS-MSN affects H_2S level in different organs. At 2 h, almost all major organs collected show elevated H_2S content, which is due to the high H_2S level in blood circulation. However, only organs accumulating nanoparticles (liver and spleen) contain more H_2S than the control at 24 h. Along with the elimination of majority DATS-MSN, the H_2S level in all organs fell to the control level at 7 d. Two measures were performed to reflect relative real condition of tissue H_2S. First, we designed a control group as the baseline. H_2S contents in liver, kidney, spleen, heart, lung and brain were all clearly elevated compared to the control group. Second, to avoid the H_2S loss from tissue samples, we also added ice-cold 5-sulfosalicylic acid into the samples to transit H_2S to HS- before measurement, which further enhanced the stability of H_2S during the measurement. Combined with MSN biodistribution, DATS-MSN is the unique H_2S donor for a slow delivery of H_2S to targeted organs after its clearance from blood circulation (such as at 24 h).

For the safety evaluation and toxicity, DATS-MSN shows a negligible cytotoxicity at the concentration required as H_2S donors, proving the biocompatibility and safety of MSN in rat cardiomyocytes. For *in vivo* safety evaluation, unlike NaHS, obvious acute adverse effects like falling blood pressure and heart rates, as well as heart inhibition were not observed in DATS-MSN. The balance of toxicity and physiological functions of H_2S depends on its concentration in the physiological environment. Our results indicated that the slow-releasing of H_2S can avoid toxicity caused by rapid increase of H_2S concentration. Although considerable liver and kidney accumulation of nanoparticles is

observed, serological examination showed that liver and kidney function are all within the normal range. In addition, hematological data show no evidence of hemolysis or inflammation. H&E staining showed no significant tissue toxicity or irreparable impairment up to 7 d, indicating that rats suffer no obvious organ toxicity. Our results preliminarily prove that the working concentration of DATS-MSN is safe both in *in vitro* and *in vivo* studies.

The short effective residence time somewhat limits the biofunction effect of H_2S. On the contrary, donors offering an accumulating H_2S circumstance over a long time period are more potent in providing therapeutic functions.[29] DATS-MSN also manifests better protection effect than free DATS, partially because of the poor solubility of DATS and its relatively fast H_2S releasing process. Therefore, DATS-MSN is exactly an ideal H_2S donor with a steady supply, to induce biofunctionality of H_2S more effectively.

Conclusions

In summary, a novel GSH-triggered, water-dispersible H_2S donor has been successfully synthesized, to slowly and controllably release moderate amounts of H_2S. DATS-MSN elevates plasma H_2S level more effectively and sustainedly compared with either NaHS or DATS. The H_2S content is elevated especially in liver and spleen, associated with the accumulation of nanoparticles in these organs. DATS-MSN can be safely used both *in vitro* and *in vivo*, and can develop a superior myocardium protection effect of H_2S from I/R injury in the cell and organ level. This study provides a consistent but tunable H_2S condition, which can be applied to *in vitro* experiments such as cytoprotection and organ preservation. This ideal MSN-based platform allows for long-range and stable releasing plasma H_2S level and distributing H_2S to targeted organs. It also provides a new insight into control-releasing various gas molecules drugs based on MSNs and MSN-based nanoparticles.

Notes

[a] *Address: Department of Cardiac Surgery, Zhongshan Hospital of Fudan University and Shanghai Institute of Cardiovascular Diseases, Shanghai 200032, P. R. China*
[b] *Address: Department of Cardiothoracic Surgery, Huashan Hospital of Fudan University, Shanghai 200040, P. R. China*
[c] *Address: Department of Chemistry, Laboratory of Advanced Materials, Shanghai 200433, P. R. China*
[d] *Address: Department of Chemical Engineering, Monash University, Clayton, Victoria 3800, Australia*
[e] *Address: Department of Cardiology, Shanghai Ninth People's Hospital, Shanghai JiaoTong University, Shanghai, 200011, P. R. China*
[f] *Address: State Key Laboratory of Molecular Engineering of Polymers and Department of Macromolecular Science, Fudan University, Shanghai, 200433, P. R. China*

** E-mail: guo.changfa@zs-hospital.sh.cn (C.F.G.), wang.chunsheng@zs-hospital.sh.cn (C.S.W.)*

† These authors contributed equally to this work.

Acknowledgements

This work was supported by the State Key Basic Research Program of the PRC (2012CB224805, 2013CB934104), the NSF of China (81270326, 51273047, 81402917, 21210004, 21322311 and 21473038), the Australian Research Council (DP120101194, DP140104062), the Deanship of Scientific Research of King Saud University (IHCRG#14-102).

References

1 D. Zhao, J. Feng, Q. Huo, N. Melosh, G.H. Fredrickson, B.F. Chmelka and G.D. Stucky, *Science*, **279**, 548-552.
2 X. Guo, Y. Deng, B. Tu and D. Zhao, *Langmuir*, 2010, **26**, 702-708.
3 S.B. Hartono, M. Yu, W. Gu, J. Yang, E. Strounina, X. Wang, S. Qiao and C. Yu, *Nanotechnology*, 2014, **25**, 055701.
4 M. Wang, Z. Sun, Q. Yue, J. Yang, X. Wang, Y. Deng, C. Yu, D. Zhao, *J. Am. Chem. Soc.*, 2014, **136**, 1884-1892.
5 J. Chen, Z. Xue, S. Feng, B. Tu, D. Zhao, *J. Colloid Interface Sci.*, 2014, **429**, 62-67.
6 Y. Chen, C. Chu, Y. Zhou, Y. Ru, H. Chen, F. Chen, Q. He, Y. Zhang, L. Zhang and J. Shi, *Small*, 2011, **7**, 2935-2944.
7 S. Jambhrunkar, Z. Qu, A. Popat, S. Karmakar, C. Xu and C. Yu. *J. Colloid Interface Sci.*, 2014, **434**, 218-225.
8 Y. Zhang, Z. Zhi, T. Jiang, J. Zhang, Z. Wang and S. Wang, *J. Controlled Release*, 2010, **145**, 257-263.
9 J. Fan, C. Yu, F. Gao, J. Lei, B. Tian, L. Wang, Q. Luo, B. Tu, W. Zhou and D. Zhao, *Angew. Chem. Int. Ed.*, 2003, **42**, 3146-3150.
10 Q. He, Z. Zhang, F. Gao, Y. Li and J. Shi, *Small*, **7**, 271-280.
11 X. Hu, X. Hao, Y. Wu, J. Zhang, X. Zhang, P. Wang, G. Zou and X. Liang, *J. Mater. Chem. B*, 2013, **1**, 1109-1118.
12 A. Popat, S. Jambhrunkar, J. Zhang, J. Yang, H. Zhang, A. Meka and C. Yu, *Chem. Commun.*, 2014, **50**, 5547-5550.
13 Y. Jiao, Y. Sun, B. Chang, D. Lu and W. Yang, *Chemistry*, 2013, **19**, 15410-15420.
14 X. Mei, S. Yang, D. Chen, N. Li, H. Li, Q. Xu, J. Ge and J. Lu, *Chem. Commun.*, 2012, **48**, 10010-10012.
15 C. Hom, J. Lu and F. Tamanoi, *J. Mater. Chem.*, 2009, **19**, 6308-6316.
16 J. Lu, M. Liong, Z. Li, J.I. Zink and F. Tamanoi, *Small*, 2010, **6**, 1794-1805.
17 M.A. Tölli, M.P. Ferreira, S.M. Kinnunen, J. Rysä, E.M. Mäkilä, Z. Szabó, R.E. Serpi, P.J. Ohukainen, M.J. Välimäki, A.M. Correia, J.J. Salonen, J.T. Hirvonen, H.J. Ruskoaho and H.A. Santos, *Biomaterials*, 2014, **35**, 8394-8405.
18 J.W. Calvert, S. Jha, S. Gundewar, J.W. Elrod, A. Ramachandran, C.B. Pattillo, C.G. Kevil and D.J. Lefer, *Circ. Res.*, 2009, **105**, 365-374.
19 N.R. Sodha, R.T. Clements, J. Feng, Y. Liu, C. Bianchi, E.M. Horvath, C. Szabo and F.W. Sellke, *Eur. J. Cardiothorac. Surg.*, 2008, **33**, 906-913.
20 G. Yang, L. Wu, B. Jiang, W. Yang, J. Qi, K. Cao, Q. Meng, A.K. Mustafa, W. Mu, S. Zhang, S.H. Snyder and R. Wang, *Science*, 2008, **322**, 587-590.
21 R.C. Zanardo, V. Brancaleone, E. Distrutti, S. Fiorucci, G. Cirino and J.L. Wallace, *FASEB J.*, 2006, **20**, 2118-2120.
22 J. Hamar, M. Solymár, E. Tanai, P. Cseplo, Z. Springo, G. Berta, B.

Debreceni and A. Koller, *Acta Physiol. Hung.*, 2012, **99**, 411-419.
23 K. Abe and H. Kimura, *J. Neurosci.*, 1996, **16**, 1066-1071.
24 M.Y. Ali, M. Whiteman, C.M. Low and P.K. Moore, *J. Endocrinol.*, 2007, **195**, 105-112.
25 S. Mani, H. Li, A. Untereiner, L. Wu, G. Yang, R.C. Austin, J.G. Dickhout, Š. Lhoták, Q.H. Meng and R. Wang, *Circulation*, 2013, **127**, 2523-2534.
26 G.L. Allison, G.M. Lowe and K. Rahman, *Life Sci.*, 2012, **91**, 1275-1280.
27 E. Blackstone, M. Morrison and M.B. Roth, *Science*, 2005, **308**, 518.
28 G. Caliendo, G. Cirino, V. Santagada and J.L. Wallace, *J. Med. Chem.*, 2010, **53**, 6275-6286.
29 L. Li, M. Whiteman, Y.Y. Guan, K.L. Neo, Y. Cheng, S.W. Lee, Y. Zhao, R. Baskar, C.H. Tan and P.K. Moore, *Circulation*, 2008, **117**, 2351-2360.
30 Q.H. Gong, Q. Wang, L.L. Pan, X.H. Liu, H. Xin and Y.Z. Zhu, Brain. *Behav. Immun.*, 2011, **25**, 110-119.
31 Y. Zhao, H. Wang and M. Xian, *J. Am. Chem. Soc.*, 2011, **133**, 15-17.
32 G.K. Kolluru, X. Shen, S.C. Bir and C.G. Kevil, *Nitric. Oxide.*, 2013, **35**, 5-20.
33 H. Amagase, *J. Nutr.*, 2006, **136**, 716S-725S.
34 G.A. Benavides, G.L. Squadrito, R.W. Mills, H.D. Patel, T.S. Isbell, R.P. Patel, V.M. Darley-Usmar, J.E. Doeller and D.W. Kraus, *Proc. Natl. Acad. Sci.*, 2007, **104**, 17977-17982.
35 M.A. Insko, T.L. Deckwerth, P. Hill, C.F. Toombs, C. Szabo, *Br. J. Pharmacol.*, 2009, **157**, 944-951.
36 D.P. Jones, J.L. Carlson, P.S. Samiec, P. Sternberg, V.C. Mody, R.L. Reed and L.A. Brown, *Clin. Chim. Acta*, 1998, **275**, 175-184.
37 II. Slowing, JL. Vivero-Escoto, C. Wu, VS. Lin, *Adv. Drug Deliv Rev.*, 2008, **60**, 1278-1288.
38 C. Cereser, J. Guichard, J. Drai, E. Bannier, I. Garcia, S. Boget, P. Parvaz and A. Revol, *J. Chromatogr. B*, 2001, **752**, 123-132.
39 F. Lu, S.H. Wu, Y. Hung and C. Mou, *Small*, 2009, **5**, 1408-1413.
40 S.H. Wu, Y.S. Lin, Y. Hung, Y.H. Chou, Y.H. Hsu, C. Chang and C. Mou, *Chembiochem*, 2008, **9**, 53-57

A table of contents entry

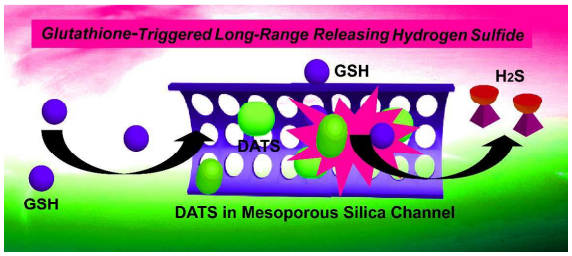

A mesoporous silica-based glutathione-triggered delivery system has been fabricated for long-range and stable releasing hydrogen sulfide.